frontiers in Marine Science

BRIEF RESEARCH REPORT
published: 16 October 2019
doi: 10.3389/fmars.2019.00636

Upwelling Amplifies Ocean Acidification on the East Australian Shelf: Implications for Marine Ecosystems

Kai G. Schulz[1]*, *Simon Hartley*[2] and *Bradley Eyre*[1]

[1] Centre for Coastal Biogeochemistry, School of Environment, Science and Engineering, Southern Cross University, Lismore, NSW, Australia, [2] Marine Ecology Research Centre, School of Environment, Science and Engineering, Southern Cross University, Lismore, NSW, Australia

Frequent upwelling of deep, cold water, rich in dissolved inorganic nutrients and carbon dioxide but low in oxygen concentrations and pH, is well documented in eastern boundary systems. As a consequence, waters in vast areas of the continental shelf can turn corrosive to the mineral aragonite, vital to a number of marine organisms. This phenomenon is projected to become more severe with ongoing ocean acidification. Although upwelling is also known to occur in western boundary systems, the impact on present day aragonite saturation state (Ω_{arag}) is virtually unknown, let alone for the decades to come. Here we identified 32 events during 18 weeks of continuous measurements in Cape Byron Marine Park, Australia, with prolonged drops in ocean temperature of up to 5°C, oxygen concentrations by 34%, pH by 0.12 and Ω_{arag} by 0.9 in a matter of hours. Temperature, salinity and oxygen saturation during these events hint at a water mass from 200 to 250 m depth off the Central East Australian shelf. Extrapolating present day upwelling to a preindustrial setting shows that ongoing ocean acidification has already lead to the crossing of a number of biological and geochemical Ω_{arag} thresholds. The future intensity of these events critically depends on carbon dioxide emission scenario, and might be even more pronounced in the Great Barrier Reef where current day shelf associated waters carry a stronger deep water signal (based on oxygen levels) than at the study location. Finally, the proposed use of artificially upwelled water to cool increasingly temperature-stressed coral reef communities will need to take its unique carbonate chemistry properties into account.

Keywords: western boundary system, upwelling, low pH, ocean acidification, Omega thresholds

OPEN ACCESS

Edited by:
Xinping Hu,
Texas A&M University Corpus Christi, United States

Reviewed by:
Wen-Chen Chou,
National Taiwan Ocean University, Taiwan
Wei-dong Zhai,
Shandong University, China

***Correspondence:**
Kai G. Schulz
kai.schulz@scu.edu.au

Specialty section:
This article was submitted to Marine Biogeochemistry, a section of the journal Frontiers in Marine Science

Received: *26 June 2019*
Accepted: *27 October 2019*
Published: *16 October 2019*

Citation:
Schulz KG, Hartley S and Eyre B (2019) Upwelling Amplifies Ocean Acidification on the East Australian Shelf: Implications for Marine Ecosystems. Front. Mar. Sci. 6:636. doi: 10.3389/fmars.2019.00636

1. INTRODUCTION

Primary productivity of marine ecosystems and resulting transfer of organic matter to higher trophic levels such as fish critically depends on the supply of dissolved inorganic nutrients. Some of the most productive regions are coasts to the Western-side of the Americas and Africa, the so-called Eastern Boundary Upwelling systems, off Chile/Peru, the United States of America, Namibia and Mauritania (Chavez and Messié, 2009; FAO, 2018). Here, the prevailing equatorward winds drive offshore Ekman transport of surface waters, leading to upwelling of deeper water masses

(Kämpf and Chapman, 2016). As a consequence of high organic matter production in the upper layer and subsequent remineralization at depth, these waters carry distinct chemical signatures of elevated nutrients and dissolved inorganic carbon concentrations, while oxygen concentrations are lowered, leading to decreased pH and calcium carbonate saturation state (Ω), and increased fugacity of carbon dioxide (fCO_2). Currently, pH as low as 7.75 (total scale) and fCO_2 levels of about 900–1,000 μatm have been reported in upwelling waters on the Californian shelf (Feely et al., 2008; Chan et al., 2017), with similar observations made during Peruvian upwelling events (Köhn et al., 2017; Chen, 2018). Under such conditions Ω will drop below 1 and waters become chemically corrosive for the calcium carbonate ($CaCO_3$) mineral aragonite, which is produced by a number of modern marine organisms such as scleractinian corals, molluscs and some sponges (Ries, 2010).

In the future ocean, upwelling events in these systems are projected to become more intense, more frequent and increase in duration (Hauri et al., 2013; Wang et al., 2015; Franco et al., 2018), although observational data hint at regional differences (Varela et al., 2015). While intensification will be driven by increasing amounts of anthropogenic CO_2 being absorbed by the world's oceans in a process termed ocean acidification (Doney et al., 2009), increases in frequency/duration are thought to be a result of enhanced land-ocean temperature gradients and alongshore winds (Di Lorenzo, 2015). Potential consequences for organisms and ecosystems include enhanced inorganic nutrient supply and increases in primary productivity, but also concomitant reductions in seawater oxygen concentrations (Di Lorenzo, 2015), with the potential to restrict pelagic fish distributions and alter predator-prey relationships (see Townhill et al., 2017 and refs. therein). Finally, further reductions in pH and Ω could decrease biogenic calcification (for a discussion on the underlying physiological drivers see Cyronak et al., 2016a,b; Waldbusser et al., 2016) in many marine taxa (Kroeker et al., 2013), increase $CaCO_3$ dissolution (Eyre et al., 2018), and hence reduce habitat suitability for calcifying organisms. In general, conditions will become more variable and extreme. This could favor a selected few of pre-adapted organisms and exclude calcifiers, which are considered keystone species in many marine ecosystems and are often of significant economic value.

While well-studied and prevalent in eastern boundary systems, upwelling of deep water also occurs in western boundary currents around the globe, mainly driven by boundary current strength, interactions with local topography, or favorable wind conditions (Roughan and Middleton, 2002; Kämpf and Chapman, 2016). In the East Australian Current (EAC) system, covering an area from north to south of more than 2,000 kilometers, upwelling has primarily been documented by rapid drops in nearshore sea surface temperatures (**Figure 1**), with typical swings lasting from hours to days and ranging from 0.5 to more than 2 $^{\circ}C$ (see refs. in **Figure 1** for details), but also by associated increases in chlorophyll *a* (e.g., Everett et al., 2014). However, the upwelling signatures in terms of carbonate chemistry speciation (pH, Ω and fCO_2) and oxygen saturation, all factors critically affecting marine organisms and ecosystems, especially in a context of ongoing ocean acidification, are virtually unknown.

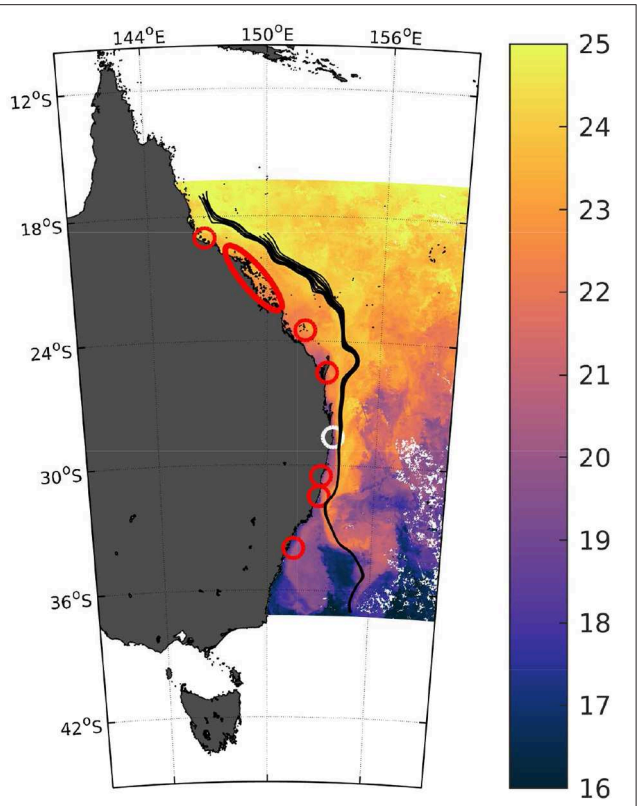

FIGURE 1 | Upwelling along the east Australian shelf. Sea surface temperatures in degrees Celsius (6 day composite) on August 18th 2017 off the East Australian coast. While the white circle marks the study location, red circles and ellipse denote areas with documented upwelling events (north to south) reported in Andrews and Furnas (1986), Oke and Middleton (2000), Roughan and Middleton (2002), Berkelmans et al. (2010), Malcolm et al. (2011), Schaeffer et al. (2013), Mao and Luick (2014), Tran et al. (2015), Wijffels et al. (2018), and Gibbs et al. (1998). The black lines highlight the continuous southwards flow of the East Australian Current in the week around August 22nd 2017 (Bonjean and Lagerloef, 2002).

2. METHODS

A SeapHOx (Sea-Bird Scientific) was deployed about 2 nautical miles offshore in a mounting frame bolted to hard substrate in 15.6 m depth in the Mackerel Boulder Habitat Protection Zone in Cape Byron Marine Park, Australia at 28.605°S and 153.629°E on August 18th 2017. The instrument was recovered for maintenance and service on October 20th 2017 and re-deployed on November 3rd 2017 until re-recovery on January 8th 2018.

2.1. Instrument Setup and Calibration

The SeapHOx is an instrument package comprising a Sea-Bird SBE 37SMP-ODO MicroCAT CTD for salinity (conductivity), temperature, and pressure, a dissolved oxygen sensor (SBE63), and an ion selective field effect transistor (ISFET) pH sensor

(Bresnahan et al., 2014). It was programmed to take six replicate recordings (consisting of 20 measurements each) in 15 min intervals. Prior to each deployment the SeapHOx was serviced, tested, and conditioned in an aerated seawater filled aquarium in a laboratory for about seven days as recommended in Bresnahan et al. (2014) and Rivest et al. (2016). For temperature, conductivity, pressure, and oxygen the factory calibration was used. Measured temperature was within 0.01°C of a NIST-certified 6412 Traceable® Platinum Ultra-Accurate digital thermometer while oxygen saturation (calculated from recorded oxygen concentration and MicroCAT temperature according to García and Gordon (1992) was measured at 96.7 ± 0.2 and 95.9 ± 0.4% for the first and second aquarium conditioning, respectively. When the laboratory air was measured for oxygen saturation in comparison to the outdoors, it was about 4% lower, hence no correction was applied to measured oxygen levels.

Calibration constants for ISFET pH against the internal and external reference electrode (**Figure S1**) were determined and calculated as described in Bresnahan et al. (2014) using the published MATLAB functions, with discrete water samples collected during deployments and recoveries, serving as the reference by providing pH_T from measured dissolved inorganic carbon (DIC) and total alkalinity (TA).

2.2. DIC and TA Measurements of Discrete Water Samples

Discrete samples for dissolved inorganic carbon (DIC) and total alkalinity (TA) during deployments and recoveries were collected next to the SeapHOx by divers into 500 ml Schott Duran glass-stoppered bottles, which were fixed with 250 μl of a saturated $HgCl_2$ solution back on shore. DIC was measured by infra-red absorption on a Marianda AIRICA equipped with a LICOR-7000 and corrected against certified reference material CRM159 (Dickson, 2010), at an overall uncertainty of 1.5 μmol kg^{-1}. TA was measured by a potentiometric open cell titration using a Metrohm 848 Titrino plus connected to a 869 Compact Sample Changer with 0.05 mol kg^{-1} HCl adjusted to a ionic strength of 0.72 mol kg^{-1} with NaCl as described in Dickson et al. (2007) and corrected against CRM159, at an overall uncertainty of 3.5 μmol kg^{-1}. DIC and TA were used together with SeapHOx derived salinity and temperature to calculate *in-situ* pH on the total scale (pH_T) using the MATLAB function CO2SYS.m (Lewis and Wallace, 1998), the dissociation constants for carbonic acid from Lueker et al. (2000), for bisulfate ion from Dickson et al. (1990), and the total boron to salinity relation from Lee et al. (2000).

2.3. Total Alkalinity Estimates, Carbonate Chemistry Speciation Calculations, and Past and Future Projections

A TA time series during the two deployments was reconstructed from a linear relationship of SeapHOx recorded salinity (assuming simple dilution or concentration as outlined in Jiang et al. (2014)) and corresponding TA measured on discrete water samples (**Figure S2**). For comparison, TA was also calculated from measured salinity and temperature as described in Lee et al. (2006). The resulting TA estimate was then used with measured pH_T (against the internal reference electrode) to calculate full carbonate chemistry speciation using the MATLAB function CO2SYS.m and the same settings as described above (see **Supplementary Methods** for a discussion of internal and external reference electrodes).

Projections of carbonate chemistry variability into the past and future were based on the assumption that advection of deep and mixing with local waters would have been or remain constant, as well as observed patterns of biological control on DIC (for details on methods and associated uncertainties see **Supplementary Methods**).

2.4. Potential Upwelling Detection and Classification

Potential upwelling events were pre-identified by scanning for continuous drops (larger than 0.25 °C) in measured temperature (also allowing for the possibility of a temperature spike with up to two data points in an overall decline - **Figure S3**). Then, the associated change in oxygen saturation state was calculated and used to narrow down actual deep water upwelling events. In this respect it is noted that corresponding changes in pH_T would have been equally suitable as of an expected highly significant ($r^2 = 0.929$, $F > 4e3$, $p << 1e\text{-}5$) correlation (**Figure S4**), suggesting mixing/replacement of oxygen-rich and high-pH warmer surface with oxygen-deficient and low-pH colder deep waters. Potential upwelling intensity was assessed in three categories of temperature according to Berkelmans et al. (2010) and also oxygen saturation changes.

3. RESULTS

During the two consecutive deployments between August 2017 and January 2018 salinity was relatively constant between 35.3 and 35.7 and there was an overall warming trend going from Austral spring into summer of about 6°C (**Figures 2A,B**). Using combined temperature and oxygen saturation decreases (see section 2 for details) as an indicator for upwelling of deep water, there were hundreds of potential candidate events (**Figure 3**). To our initial surprise, the correlation between temperature and oxygen saturation drops was relatively poor in terms of predictive power ($r^2 = 0.285$), although statistically significant ($F = 52$, $p << 1e\text{-}5$). However, this is expected if the deep water source being upwelled remains the same throughout the year. Then, for the same drop in oxygen saturation in an upwelling event the drop in temperature will depend on initial surface ocean conditions (assuming quasi air-sea O_2 equilibrium in these oligotrophic waters) and be larger in summer than in winter/spring. This is indeed what appears to have happened (**Figure 3**).

Using temperature only as an indicator for upwelling and its intensity like in previous studies (Berkelmans et al., 2010), there would have been 102 events of low (ΔTemperature between –0.5 and –1°C), 62 of medium (between –1 and –2°C) and 54 of high intensity (beyond –2°C). In contrast, when

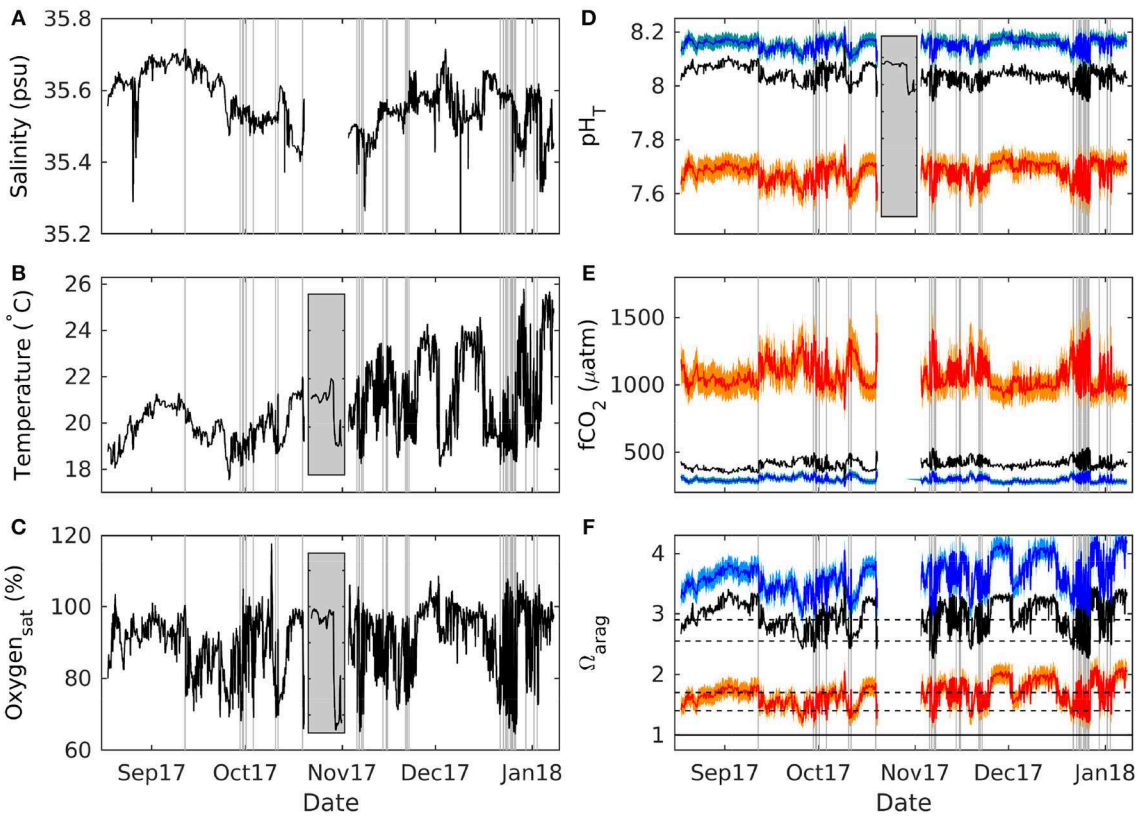

FIGURE 2 | Measured present day, and calculated preindustrial and future upwelling. Variability in measured salinity **(A)**, temperature **(B)**, oxygen saturation **(C)**, and pH on the total scale **(D)**, together with calculated CO_2 fugacity **(E)** and aragonite saturation state **(F)** at the mooring site in Cape Byron Marine Park. Black lines illustrate measurements between August 18th 2017 and January 8th 2018, while blue and red lines denote estimated variability for a preindustrial and future (RCP8.5) ocean, respectively, with lighter colors highlighting uncertainty bounds (see Methods for details on calculations). Gray vertical lines denote all major upwelling events (see text for details). The gray insets in **(B–D)** present a close up of temperature, oxygen and pH changes during an upwelling event on the last 2 days of the first deployment. Black horizontal lines in **(F)** denote various aragonite saturation state thresholds (see text and **Table 1** for details).

accompanying changes in oxygen saturation are used as such proxy there were about 30% less potential candidate events (**Figure 3**). Tentatively grouping them in terms of intensity, there were 71 of low (between −5 and −10%), 52 of medium (between −10 and −20%) and 32 of high intensity (beyond −20%). For example, one of the larger events at the end of the first instrument deployment was characterized by drops in temperature of ∼3°C and oxygen saturation by ∼30% within a few hours (**Figures 2B,C**, **Figure S3**). Corresponding changes in carbonate chemistry speciation were drops in pH by ∼0.11, in Ω_{arag} by ∼0.8 and an increase in fCO_2 by ∼135 μatm (**Figures 2D–F**, **Figure S3**).

4. DISCUSSION

4.1. Origin of Upwelled Deep Water

The observation that temperature drops during potential upwelling events tend to be larger in summer, when initial surface temperatures are warmer than in winter/spring (**Figure 3**), could be explained by upwelling of certain deep water with particular water mass characteristics. While temperature and salinity varied relatively substantially throughout the two deployments, ranging between ∼18–26°C and ∼35.3–35.7, respectively, they were relatively constant at the end of the potential upwelling events of high intensity (in terms of oxygen saturation changes, i.e., beyond −20%), with 18.87 ± 0.58°C and 35.54 ± 0.04 (**Figure S5**). According to the World Ocean Atlas, this T-S relationship is characteristic of waters in front of the Central East Australian Shelf, in close proximity to the mooring site, at depths between 200 and 250 m (compare **Figures 4A,B** and **Figures S6A,B**). The average oxygen saturation level of this water mass of 81.5 ± 2.0% (**Figure 4C**, **Figure S6C**) was slightly higher than the average of 74.4 ± 4.3% measured at the end of the 32 (**Figure 3**) candidate events of high intensity (in terms of oxygen saturation changes). This offset could be the results of a much lower number of observations for oxygen in comparison to temperature and salinity in this region, which could mask local variability. There are indeed a number of individual Argo (Argo, 2000) float measurements (float identifier 5905165, downloaded from http://imos.org.au/facilities/argo/) in this area from 2016 that show oxygen

saturation levels down to 70% in 200–250 m depth (data not shown).

In summary, the relatively uniform combination of salinity, temperature and oxygen saturation at the end of the 32 high intensity events identified by our analysis (**Figure 3**, **Figure S5**) points towards the upwelling of a water mass that is sitting directly in front of the Central east Australian shelf in a depth of 200–250 m.

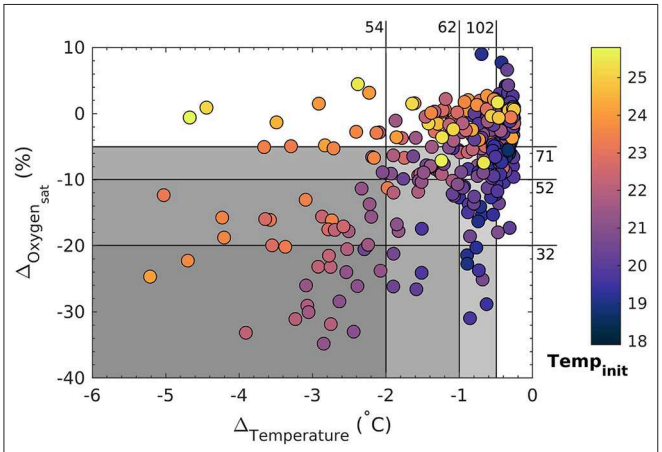

FIGURE 3 | Temperature and oxygen saturation drops in the context of initial temperatures. Measured temperature and concomitant oxygen saturation changes during events of rapid and sustained drops at three temperature and oxygen intensity ranges (gray). Shown are all events with a temperature drop larger than 0.25°C, while the color code denotes initial temperatures. The numbers on the top and to the right are a count of the events inside each respective range (see text for details).

4.2. Identifying and Classifying Upwelling Events

While the 32 events of high intensity (in terms of oxygen saturation changes) appear to be the result of the upwelling of a unique deep water mass, the 54 candidate events of high intensity (in terms of temperature changes) contain some that clearly do not qualify as deep water upwelling. These are in particular those with no or hardly any associated oxygen saturation change (**Figure 3**). As their oxygen saturation is close to air-sea equilibrium, the temperature drop might be the result of more southerly coastal surface waters that had been pushed north (**Figure 4B**).

In essence, temperature changes alone are not necessarily a robust indicator of deep water upwelling (at least at this location). They are also not a good proxy for upwelling intensity, and significant events (in terms of oxygen and associated carbonate chemistry speciation changes) can escape detection, especially in colder winter months when local sea temperatures are close to those of the water mass being upwelled (**Figure 3**).

Taking again oxygen saturation changes as a better upwelling indicator, the potential events of medium intensity most likely encompass two types. The first is incomplete upwelling and partial mixing with local waters, reducing the magnitude of overall observed changes. The second is probably the upwelling of waters from shallower depths. This might have happened at the event in early December, when temperatures dropped about 5°C (compare **Figure 2B**), as the combination of the associated

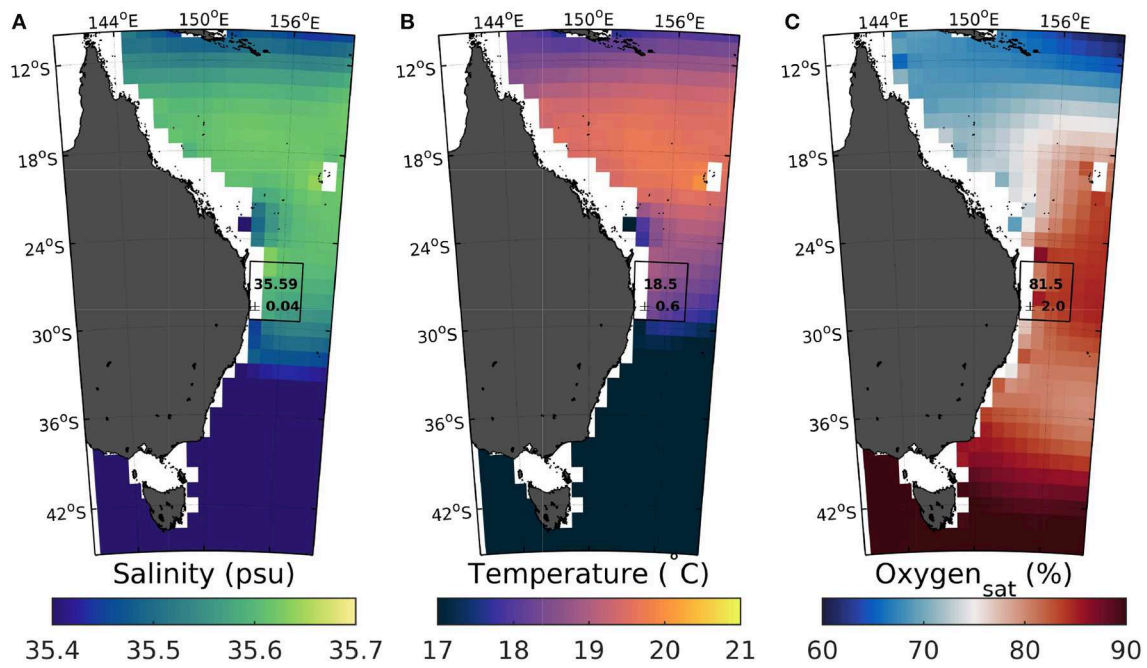

FIGURE 4 | Salinity, temperature, and oxygen saturation climatologies in 200–250 m depth. Mean (200–250 m depth) annual World Ocean Atlas 2009 climatologies of salinity **(A)**, temperature **(B)**, and oxygen saturation **(C)** off the Australian east coast (Antonov et al., 2010; Garcia et al., 2010; Locarnini et al., 2010). Numbers in black squares denote the respective 4 × 4 grid point averages and standard deviations (between 25.5–29.5°S and 153.5–157.5°E).

oxygen saturation drop by ∼12% and the increase to a salinity of 35.6 is indicative of a shallower water mass (**Figure S6**).

In summary, during the 18 weeks of deployment, there were 32 events of deep water upwelling of high intensity (from 200 to 250 m depth) and additional potential 52 of medium intensity, including partial upwelling and/or from shallower depths.

4.3. Past, Present and Future Carbonate Chemistry Variability

Seawater carbonate chemistry speciation can vary considerably during upwelling events. During those of high intensity (in terms of oxygen saturation changes) measured average pH dropped by ∼0.8, and calculated fCO_2 rose by ∼100 μatm while aragonite saturation state (Ω_{arag}) decreased by ∼0.65. Concerning the latter, there are a number of critical geochemical and physiological thresholds. While at a seawater $\Omega_{arag} < 1$ aragonite will start to dissolve, it has been found that sediments turn from net precipitating to net dissolving already at much higher saturation state in the overlying water column of 2.9 (Eyre et al., 2018). This is the result of benthic heterotrophy that drives pore water undersaturation. On the ecosystem level, when combining the impacts of seawater carbonate chemistry on sediment dissolution with reported impacts on biogenic calcification, the same study estimated reefs (with a 95% sediment and 5% coral cover) to transition to net dissolving below a seawater Ω_{arag} of 2.55 (Eyre et al., 2018). While we calculate none of these thresholds to have been crossed at our study location in a preindustrial setting at overall lower atmospheric fCO_2 (see section 2 for details), at the present day seawater aragonite saturation state is below 2.9 and 2.55 for 40% and 7% of the time, respectively (compare **Figure 2** and **Table 1**). An increase of atmospheric fCO_2 to 985 μatm, as projected by the RCP8.5 scenario until the end of this century (IPCC, 2013), would see this location below both the 2.9 and 2.55 thresholds permanently (compare **Figure 2** and **Table 1**). Furthermore, for 54% and 10% of the time it would be below 1.7 and 1.4, which mark oyster larvae net growth to equal mortality and the start of pteropod shell dissolution, respectively (see McLaughlin et al., 2018 and references therein). Regardless of the exact species-specific thresholds and atmospheric CO_2 concentrations to be reached in the future, it becomes evident that a number of important geochemical and biological processes will be progressively affected, having the potential to drive changes on the ecosystem level.

4.4. Upwelling Along the East Australian Shelf

The rapid swings in temperature and frequency recorded here (between 0.5–5°C) are comparable to those reported previously along the east Australian shelf. Depending on location, upwelling can be driven by wind, EAC encroachment onto the shelf, EAC acceleration, or EAC separation from the coast (Roughan and Middleton, 2002). And although there are large stretches of coastline without documented upwelling, there are still relatively large areas such as in the central and southern Great Barrier Reef where upwelling occurs at least seasonally (see **Figure 1** and references therein). If there the depth from which deep water is being upwelled is similar to our study location, drops in oxygen saturation and hence associated changes in carbonate chemistry speciation could be even more pronounced further north, with the former being up to one third lower (**Figure 4C**).

Furthermore, the flow of deep water onto the shelf can also remain confined to the bottom (Wijffels et al., 2018), making detection difficult, yet having the potential to impact benthic communities. Overall, this suggests that significant variability in oxygen, pH, and associated $CaCO_3$ saturation states might be a common and, until now, a completely overlooked phenomenon along Australia's East coast (and potentially Western Boundary Upwelling systems globally).

TABLE 1 | Temporal extent (%) of Ω_{arag} below a range of geochemical and physiological thresholds.

Ω_{arag}	Current day (%)	Pre-Ind. (%)	RCP 2.6 (%)	RCP 4.5 (%)	RCP 8.5 (%)
2.9	40	0	68	95	100
2.55	7	0	21	61	100
1.7	0	0	0	0	54
1.4	0	0	0	0	10
1.0	0	0	0	0	0

Relative time of aragonite saturation levels below certain thresholds during the 18 week deployment period was calculated for present and preindustrial conditions, and peak atmospheric CO_2 levels until the end of this century according to various Representative Concentration Pathways (see text and methods for details).

4.5. Potential Changes to Future Upwelling Frequency and Duration

Future swings in coastal carbonate chemistry speciation and oxygen as shown here would further be enhanced when frequency and duration of upwelling events increase. This could be a consequence of changes to EAC flow which, in the past few decades, has increased its southward penetration (Ridgway, 2007) and is projected to further intensify, both in terms of water transport and extension (Sun et al., 2011). Hence, it is paramount to start monitoring upwelling events, especially in sensitive key areas dominated by aragonite producing organisms such as the Great Barrier Reef along the East Australian coast, and assess their impact in terms of combined changes in temperature, nutrients, oxygen, pH and Ω_{arag}, not only on the organismal but also ecosystem level. This is of particular importance if artificial upwelling is to be used to cool surface waters, which has been suggested as a potential solution to provide a thermal refuge for increasingly temperature-stressed coral reef communities.

DATA AVAILABILITY STATEMENT

All time series data has been made available in the PANGAEA open repository (doi: 10.1594/PANGAEA.905880).

AUTHOR CONTRIBUTIONS

KS conceived the study, performed the field work and data analysis, and wrote the manuscript. SH performed the field work and contributed to writing. BE conceived the study and contributed to writing.

FUNDING

Funding was provided by the Australian Research Council grants FT120100384 awarded to KS and DP150102092 awarded to KS and BE.

ACKNOWLEDGMENTS

Sea surface temperature data (IMOS - SRS Satellite - SST L3S - 06 day composite - day time) was sourced from the Integrated Marine Observing System (IMOS) - IMOS is a national collaborative research infrastructure, supported by the Australian Government (https://portal.aodn.org.au/search). Current data was sourced from OSCAR third degree resolution ocean surface currents. Ver. 1. PO.DAAC, CA, USA, and the dataset was accessed [2018-06-06] at http://dx.doi.org/10.5067/OSCAR-03D01. Field work in Cape Byron Marine Park was undertaken under Marine Parks Permit # OUT17/14019. Marine Parks staff are thanked for providing support and assistance in undertaking this research. We also acknowledge Blue Bay Divers, and Dirk Erler, Natsha Gafar, Laura Stoltenberg, and Tom Glaze for their assistance in SeapHOx deployment and recovery. Last but not least we gratefully acknowledge Toste Tanhua (GEOMAR) for sharing his insights regarding estimating uncertainties in anthropogenic CO_2 calculations.

SUPPLEMENTARY MATERIAL

The Supplementary Material for this article can be found online at: https://www.frontiersin.org/articles/10.3389/fmars.2019.00636/full#supplementary-material

REFERENCES

Andrews, J. A., and Furnas, M. J. (1986). Subsurface intrusions of Coral Sea water into the central Great Barrier Reef - I. Sturctures and shelf-scale dynamics. *Cont. Shelf Res.* 6, 491–514. doi: 10.1016/0278-4343(86)90020-8

Antonov, J. I., Seidov, D., Boyer, T. P., Locarnini, R. A., Mishonov, A. V., and Garcia, H. E. (2010). *World Ocean Atlas 2009, Volume 2: Salinity. S. Levitus, Ed.* Washington, DC: NOAA Atlas NESDIS 69, U.S. Government Printing Office.

Argo (2000). Argo float data and metadata from Global Data Assembly Centre (Argo GDAC). *SEANOE*. doi: 10.17882/42182

Berkelmans, R., Weeks, S. J., and Steinberg, C. R. (2010). Upwelling linked to warm summers and bleaching on the Great Barrier Reef. *Limnol. Oceanogr.* 55, 2634–2644. doi: 10.4319/lo.2010.55.6.2634

Bonjean, F., and Lagerloef, G. S. E. (2002). Diagnostic model and analysis of the surface currents in the tropical Pacific Ocean. *J. Phys. Oceanogr.* 32, 2938–2954. doi: 10.1175/1520-0485(2002)032<2938:DMAAOT>2.0.CO;2

Bresnahan, P. J., Martz, T. R., Takeshita, Y., Johnson, K. S., and LaShomb, M. (2014). Best practices for autonomous measurement of seawater pH with the Honeywell Durafet. *Methods Oceanogr.* 9, 44–60. doi: 10.1016/j.mio.2014.08.003

Chan, F., Barth, J. A., Blanchette, C. A., Byrne, R. H., Chavez, F., Cheriton, O., et al. (2017). Persistent spatial structuring of coastal ocean acidification in the California Current System. *Sci. Rep.* 7:2526. doi: 10.1038/s41598-017-02777-y

Chavez, F., and Messié, M. (2009). A comparison of eastern boundary upwelling ecosystems. *Progr. Oceanogr.* 83, 80–96. doi: 10.1016/j.pocean.2009.07.032

Chen, S. (2018). *The development of sea surface carbonate chemistry in the coastal upwelling area off Peru following a simulated OMZ upwelling event* (Master's Thesis). Kiel University, Kiel, Germany.

Cyronak, T., Schulz, K. G., and Jokiel, P. L. (2016a). Response to Waldbusser et al. (2016): 'Calcium carbonate saturation state: on myths and this or that stories'. *ICES J. Mar. Sci.* 73, 569–571. doi: 10.1093/icesjms/fsv224

Cyronak, T., Schulz, K. G., and Jokiel, P. L. (2016b). The Omega myth: what really drives lower calcification rates in an acidifying ocean. *ICES J. Mar. Sci.* 73, 558–562. doi: 10.1093/icesjms/fsv075

Di Lorenzo, E. (2015). The future of coastal ocean upwelling. *Nature* 518, 310–311. doi: 10.1038/518310a

Dickson, A. G. (2010). Standards for ocean measurements. *Oceanogr.* 23, 34–47. doi: 10.5670/oceanog.2010.22

Dickson, A. G., Sabine, C. L., and Christian, J. E. (2007). Guide to best practices for ocean CO_2 measurements. *Spec. Publ.* 3:191.

Dickson, A. G., Wesolowski, D. J., Palmer, D. A., and Mesmer, R. E. (1990). Dissociation constant of bisulfate ion in aqueous sodium chloride solutions to 250 °C. *J. Phys. Chem.* 94, 7978–7985. doi: 10.1021/j100383a042

Doney, S. C., Fabry, V. J., Feely, R. A., and Kleypas, J. A. (2009). Ocean acidification: the other CO_2 problem. *Annu. Rev. Mar. Sci.* 1, 169–192. doi: 10.1146/annurev.marine.010908.163834

Everett, J. D., Baird, M. E., Roughan, M., Suthers, I. M., and Doblin, M. A. (2014). Relative impact of seasonal and oceanographic drivers on surface chlorophyll a along a western boundary current. *Progr. Oceanogr.* 120, 340–351. doi: 10.1016/j.pocean.2013.10.016

Eyre, B. D., Cyronak, T., Drupp, P., De Carlo, E. H., Sachs, J. P., and Andersson, A. J. (2018). Coral reefs will transition to net dissolving before end of century. *Science* 359, 908–911. doi: 10.1126/science.aao1118

FAO (2018). *The State of World Fisheries and Aquaculture 2018 - Meeting the Sustainable Development Goals*. Rome: Food and Agriculture Organization of the United Nations.

Feely, R. A., Sabine, C. L., Hernandez-Ayon, J. M., Ianson, D., and Hales, B. (2008). Evidence for upwelling of corrosive 'acidified' water onto the continental shelf. *Science* 320, 1490–1492. doi: 10.1126/science.1155676

Franco, A. C., Gruber, N., Frölicher, T. L., and Kropuenske Artman, L. (2018). Contrasting impact of future CO_2 emission scenarios on the extent of $CaCO_3$ mineral undersaturation in the humboldt current system. *J. Geophys. Res. Oceans* 123, 2018–2036. doi: 10.1002/2018JC013857

García, H. E., and Gordon, L. I. (1992). Oxygen solubility in seawater: better fitting equations. *Limnol. Oceanogr.* 37, 1307–1312. doi: 10.4319/lo.1992.37.6.1307

Garcia, H. E., Locarnini, R. A., Boyer, T. P., and Antonov, J. I. (2010). *World Ocean Atlas 2009, Volume 3: Dissolved Oxygenn, Apparent Oxygen Utilization, and Oxygen Saturation. S. Levitus, Ed.* Washington, DC: NOAA Atlas NESDIS 70, U.S. Government Printing Office.

Gibbs, M. T., Middleton, J. H., and Marchesiello, P. (1998). Baroclinic response of Sydney shelf waters to local wind and deep ocean forcing. *J. Phys. Oceanogr.* 28, 178–190.

Hauri, C., Gruber, N., McDonnell, A. M. P., and Vogt, M. (2013). The intensity, duration, and severity of low aragonite saturation state events on the california continental shelf. *Geophys. Res. Lett.* 40, 3424–3428. doi: 10.1002/grl.50618

IPCC (2013). "Annex II: climate system scenario tables," in *Climate Change 2013: The Physical Science Basis. Contribution of Working Group I to the Fifth Assessment Report of the Intergovernmental Panel on Climate Change*, eds T. F. Stocker, D. Qin, G.-K. Plattner, M. Tignor, S. K. Allen, J. Boschung, A. Nauels, Y. Xia, V. Bex, and P.M. Midgley (Cambridge; New York, NY: Cambridge University Press), 1535. doi: 10.1017/CBO9781107415324

Jiang, Z. P., Tyrell, T., Hydes, D. J., Dai, M., and Hartman, S. E. (2014). Variability of alkalinity and the alkalinity-salinity relationship in the tropical and subtropical surface ocean. *Glob. Biogeochm. Cycles* 28, 729–742. doi: 10.1002/2013GB004678

Kämpf, J., and Chapman, P. (2016). "The functioning of coastal upwelling systems," in *Upwelling Systems of the World* (Springer International Publishing), 31–66.

Köhn, E. E., Thomson, S., Arévalo-Martínez, D. L., and Kanzow, T. (2017). Submesoscale CO_2 variability across an upwelling front off Peru. *Ocean Sci.* 13, 1017–1033. doi: 10.5194/os-13-1017-2017

Kroeker, K. J., Kordas, R. L., Crim, R., Hendriks, I. E., Ramajo, L., Singh, G. S., et al. (2013). Impacts of ocean acidification on marine organisms: quantifying sensitivities and interaction with warming. *Glob. Change Biol.* 19, 1884–1896. doi: 10.1111/gcb.12179

Lee, K., Kim, T., Byrne, R., Millero, F., Feely, R., and Liu, Y. (2000). The universal ratio of boron to chlorinity for the north pacific and north atlantic oceans. *Geochim. Cosmochim. Acta* 74, 1801–1811. doi: 10.1016/j.gca.2009.12.027

Lee, K., Tong, L. T., Millero, F. J., Sabine, C. L., Dickson, A. G., Goyet, C., et al. (2006). Global relationships of total alkalinity with salinity and temperature in surface waters of the world's oceans. *Geophys. Res. Lett.* 33:L19605. doi: 10.1029/2006GL027207

Lewis, E., and Wallace, D. W. R. (1998). *Program Developed for* CO_2 *System Calculations. ORNL/CDIAC-105*. Oak Ridge, TN: Carbon Dioxide Information Analysis Center, Oak Ridge National Laboratory, U.S. Department of Energy.

Locarnini, R. A., Mishonov, A. V., Antonov, J. I., Boyer, T. P., and Garcia, H. E. (2010). *World Ocean Atlas 2009, Volume 1: Temperature*. ed S. Levitus. Washington, DC: NOAA Atlas NESDIS 68, U.S. Government Printing Office.

Lueker, T. J., Dickson, A. G., and Keeling, C. D. (2000). Ocean pCO_2 calculated from dissolved inorganic carbon, alkalinity, and equations for K_1 and K_2: validation based on laboratory measurements of CO_2 in gas and seawater at equilibrium . *Mar. Chem.* 70, 105–119. doi: 10.1016/S0304-4203(00)00022-0

Malcolm, H. A., Davies, P. L., Jordan, A., and Smith, S. D. A. (2011). Variation in sea temperature and the East Australian Current in the Solitary Islands region between 2001—2008. *Deep Sea Res. II* 58, 616–627. doi: 10.1016/j.dsr2.2010.09.030

Mao, Y., and Luick, J. (2014). Circulation in the southern Great Barrier Reef studied through an integration of multiple remote sensing and *in situ* measurements. *J. Geophys. Res. Oceans* 119, 1621–1643. doi: 10.1002/2013JC009397

McLaughlin, K., Nezlin, N. P., Weisberg, S. B., Dickson, A. G., Booth, J. A. T., Cash, C. L., et al. (2018). Seasonal patterns in aragonite saturation state on the southern california continental shelf. *Cont. Shelf Res.* 167, 77–86. doi: 10.1016/j.csr.2018.07.009

Oke, P. R., and Middleton, J. H. (2000). Topographically induced upwelling off Eastern Australia. *J. Phys. Oceanogr.* 30, 512–531. doi: 10.1175/1520-0485(2000)030<0512:TIUOEA>2.0.CO;2

Ridgway, K. R. (2007). Long-term trend and decadal variability of the southward penetration of the East Australian Current. *Geophys. Res. Lett.* 34:L13613. doi: 10.1029/2007GL030393

Ries, J. B. (2010). Review: geological and experimental evidence for secular variation in seawater Mg/Ca (calcite-aragonite seas) and its effects on marine biological calcification. *Biogeoscience* 7, 2795–2849. doi: 10.5194/bg-7-2795-2010

Rivest, E. B., O'Brien, M., Kapsenberg, L., Gotschalk, C. C., Blanchette, C. A., Hoshijima, U., et al. (2016). Beyond the benchtop and the benthos: dataset management planning and design for time series of ocean carbonate chemistry associated with Durafet®-based pH sensors. *Ecol. Informat.* 36, 209–220. doi: 10.1016/j.ecoinf.2016.08.005

Roughan, M., and Middleton, J. H. (2002). A comparison of observed upwelling mechanisms off the east coast of Australia. *Cont. Shelf Res.* 22, 2551–2572. doi: 10.1016/S0278-4343(02)00101-2

Schaeffer, A., Roughan, M., and Morris, B. D. (2013). Cross-shelf dynamics in a Western boundary current regime: implications for upwelling. *J. Phys. Oceanogr.* 43, 1042–1059. doi: 10.1175/JPO-D-12-0177.1

Sun, C., Feng, M., Matear, R. J., Chamberlain, M. A., Craig, P., Ridgway, K. R., et al. (2011). Marine downscaling of a future climate scenario for australian boundary currents. *J. Clim.* 25, 2947–2962. doi: 10.1175/JCLI-D-11-00159.1

Townhill, B. L., Pinnegear, J. K., Righton, D. A., and Metcalfe, J. D. (2017). Fisheries, low oxygen and climate change: how much do we really know? *J. Fish Biol.* 90, 723–750. doi: 10.1111/jfb.13203

Tran, D. V., Gabric, A., and Cropp, R. (2015). Interannual variability in chlorophyll-a on the southern Queensland continental shelf and its relationship to ENSO. *J. Sea Res.* 106, 27–38. doi: 10.1016/j.seares.2015.09.007

Varela, R., Álvarez, I., Santos, F., deCastro, M., and Gómez-Gesteira, M. (2015). Has upwelling strengthened along worldwide coasts over 1982-2010? *Sci. Rep.* 5:10016. doi: 10.1038/srep10016

Waldbusser, G., Hales, B., and Haley, B. A. (2016). Calcium carbonate saturation state: on myths and this or that stories. *ICES J. Mar. Sci.* 73, 569–571. doi: 10.1093/icesjms/fsv174

Wang, D., Gouhier, T. C., Menge, B. A., and Ganguly, A. R. (2015). Intensification and spatial homogenization of coastal upwelling under climate change. *Nature* 518, 390–394. doi: 10.1038/nature14235

Wijffels, S. E., Beggs, H., Griffin, C., Middleton, J. F., Cahill, M., King, E., et al. (2018). A fine spatial-scale sea surface temperature atlas of the Australian regional seas (SSTAARS): Seasonal variability and trends around Australasia and New Zealand revisited. *J. Mar. Syst.* 187, 156–196. doi: 10.1016/j.jmarsys.2018.07.005

Conflict of Interest: The authors declare that the research was conducted in the absence of any commercial or financial relationships that could be construed as a potential conflict of interest.